Transient Vortex States in $Bi_2Sr_2CaCu_2O_{8+\delta}$ Crystals

D. Giller,[1] A. Shaulov,[1] T. Tamegai,[2] and Y. Yeshurun[1]
[1]*Institute of Superconductivity, Bar-Ilan University, Ramat-Gan 52900, Israel*
[2]*Department of Applied Physics, The University of Tokyo, Hongo, Bunkyo-ku, Tokyo 113-8656, Japan*
(Received 29 November 1999)

A high temporal resolution magneto-optical system is employed to observe the time evolution of the vortex structure in $Bi_2Sr_2CaCu_2O_{8+\delta}$ crystals after a sudden application of a magnetic field. The magneto-optical images reveal dynamic coexistence of two vortex phases: a quasiordered phase in the sample interior and a transient disordered phase near the sample edges. The border between these two phases, marked by an abrupt change in the gradient of the local induction, moves with time. This motion enables tracing the decay of the transient state and the concurrent growth of the thermodynamic vortex phases. The growth rate is sensitive to the location in the field-temperature phase diagram.

PACS numbers: 74.60.Ge, 64.60.My, 74.72.Hs

The thermodynamic phase diagram of the vortex matter in high-temperature superconductors is a topic of extensive theoretical and experimental research. Most efforts have been concentrated on the highly anisotropic $Bi_2Sr_2CaCu_2O_{8+\delta}$ (BSCCO) crystals, revealing a rich phase diagram. In particular, neutron scattering [1] and μSR [2] experiments revealed the existence of two distinct vortex solid phases: a quasiordered lattice at low fields and a highly disordered solid at high fields. The transition between these two phases is manifested in magnetic measurements as a sharp increase in the persistent current density [3–8]. A problem of fundamental interest is the process of formation of the various vortex phases following a sudden change in the thermodynamic conditions (e.g., temperature T or induction B). Tracing the formation of the various vortex phases is expected to shed light on the nucleation and growth of these phases—processes that so far have hardly been explored.

In this paper we focus on the two vortex solid phases in BSCCO. Utilizing a high temporal resolution magneto-optical method for direct flux visualization, we follow the time evolution of the vortex structure in BSCCO after a sudden increase in the applied magnetic field, causing the induction field B_a at the sample edge to be smaller or larger than the transition field B_{ss} between the two solid vortex phases. In both cases the images reveal a dynamic coexistence of two distinct vortex phases: a quasiordered phase in the sample interior and a disordered phase near the sample edges. The border between these two phases, marked by a sharp change in the gradient of the local induction, moves in different modes, depending on the relation between B_a and B_{ss}. This motion enables tracing the evolution of the thermodynamic quasiordered and disordered vortex phases in early stages of their formation.

The study was carried out on two BSCCO single crystals, referred to as S1 ($0.66 \times 0.24 \times 0.03$ mm^3, $T_c \approx 80$ K) and S2 ($1.5 \times 0.68 \times 0.03$ mm^3, $T_c \approx 88$ K), which were grown using the traveling solvent floating zone method [9]. In the temperature range of the experiments described below, B_{ss}, as measured from the onset of the second magnetization peak [10], is approximately 380 and 460 G for S1 and S2, respectively [7]. The normal component of the magnetic induction B was detected on the sample's surface employing magneto-optically active ferrimagnetic iron-garnet films with in-plane magnetization [8,11]. Polarized light passing through the indicator changes its angle of polarization as a function of the local magnetic induction. Measurements were performed immediately after a sudden application of the external field H_a (rise time ≈ 50 ms), parallel to the c axis and perpendicular to the sample's surface. More than 100 two-dimensional images were then captured by a CCD video camera at time intervals of 40 ms. From these images, one-dimensional profiles (induction vs position) across the sample width were extracted.

Figure 1 shows the time evolution of the magnetic induction profiles in sample S1 at $T = 23$ K, after a sudden increase of the external magnetic field from zero to 350 Oe. Surface currents result in the sharp induction step observed at the edges [12], reducing the edge

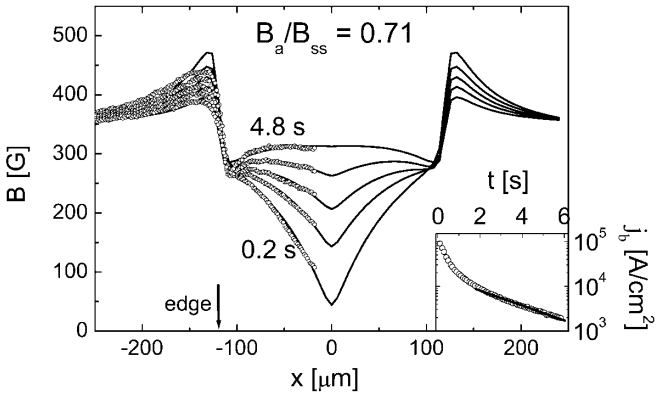

FIG. 1. Time evolution of the magnetic induction profiles for field $H_a = 350$ Oe ($B_a = 270$ G, $B_a/B_{ss} = 0.71$), for sample S1. Profiles shown are measured at $t = 0.2$, 0.32, 0.6, 1.2, and 4.8 s. Solid lines are theoretical fits with bulk current density j_b and surface current density j_s as parameters. Inset: Semilog plot of j_b vs time. Solid line indicates the exponential tail.

 0031-9007/00/84(16)/3698(4)$15.00

induction to $B_a \approx 270$ G, corresponding to $B_a/B_{ss} \approx 0.71$. In the long time limit, a dome-shaped profile, characteristic of surface and geometrical barriers in thin samples [13], is observed. Since $B < B_{ss}$ throughout the sample, the dome-shaped profile implies the establishment of a quasiordered stable state with vanishing bulk current density j_b. The time dependence of j_b, as deduced from fits of the profiles employing the Biot-Savart law, is shown in the semilog plot in the inset. It exhibits unconventional creep behavior, with an exponential tail indicated by the solid line in the inset [14].

The data of Fig. 1 show no evidence for the coexistence of different vortex phases in different parts of the sample. An evidence for such a situation is observed when B_a is closer to B_{ss}. Figure 2 shows the time evolution of the magnetic induction profiles in sample S2 at $T = 20$ K after a step increase of the external magnetic field, from zero to 470 Oe, yielding $B_a/B_{ss} \approx 0.98$. A striking feature in Fig. 2 is the sharp change in the slope of the induction profiles at $x = x_f$ (marked by bold circles). As evident from the figure, the point x_f moves progressively with time toward the sample edges ($|x| = w/2$) and, simultaneously, the induction B_f at x_f increases. (Note that initially B_f is well below B_{ss}.) In the following we show that remarkable changes in the bulk current density and in the magnetic relaxation characteristics occur at the point x_f. We first note that in contrast to the profiles shown in Fig. 1, the profiles of Fig. 2 cannot be reasonably fitted to the Biot-Savart law using a uniform bulk current density. However, assuming two different values, j_h and j_l, for the bulk current density on both sides of x_f, one obtains excellent fit as shown by the solid lines in Fig. 2 [15]. The log-log plot in the lower inset of Fig. 2 shows

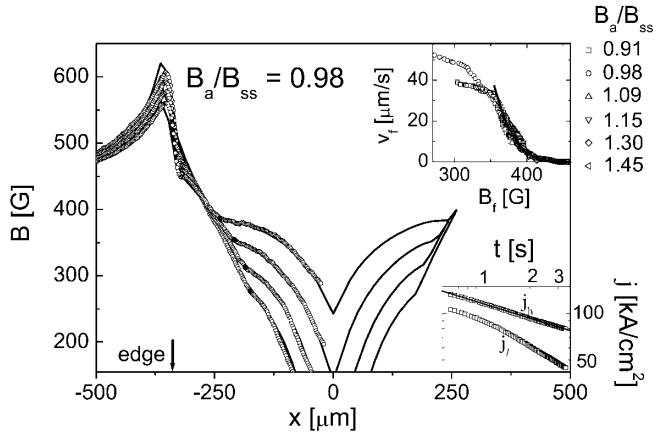

FIG. 2. Time evolution of the magnetic induction profiles for field $H_a = 470$ Oe ($B_a = 450$ G, $B_a/B_{ss} = 0.98$), for sample S2. Profiles shown are measured at $t = 0.62$, 1.02, 1.75, and 3.47 s. Solid lines are theoretical fits, with j_s, j_l, j_h, and x_f as fitting parameters. Bold circles denote the location x_f of the breaks in the profiles, deduced from the fits. Lower inset: Log-log plot of $j_h(t)$ and $j_l(t)$. Solid line: Fit of power law for j_h, with an exponent -0.31. Upper inset: v_f vs B_f for the indicated inductions. Solid line: Fit to $v_f = 0.95 \times (1 - B_f/460)^{3.75}$.

that the bulk current density j_h, corresponding to the part of the profile near the edges, exhibits a power-law decay with time ($j_h \propto t^{-0.31}$, solid line in the inset), whereas deviations from a power law are evident for $j_l(t)$. The power-law decay observed for $j_h(t)$ implies logarithmic divergence of the activation energy for flux creep as the current density approaches zero [16,17]. This behavior is characteristic of the disordered (glassy) vortex state with plastic creep [10,18,19]. The appearance of the break point x_f and its motion toward the sample edge are also observed in sample S1. Nevertheless, we chose to demonstrate these phenomena in the larger sample S2, because the motion of x_f in this sample can be followed over significantly larger distance.

Similar breaks in the induction profiles are also obtained for a sudden increase of B_a to above B_{ss}. For example, in Fig. 3 we show the time evolution of the magnetic induction profiles for sample S1 at $T = 23$ K, after a step increase of H_a from zero to 510 Oe, corresponding to $B_a/B_{ss} = 1.13$. Sharp changes in the slope of the profiles (at break points marked by bold circles) are evident. Similar to the previous case, the relaxation on both sides of the break point is governed by different laws, as illustrated in the log-log plot in the inset. The intriguing observation in Fig. 3 is that the motion of the break point is nonmonotonic: Initially, it moves toward the edges; however, at some point it changes direction and starts moving backwards, toward the sample center. During this nonmonotonic motion, the induction B_f at x_f continuously increases. The different modes of motion of x_f are summarized for sample S1 in Fig. 4 as plots of B_f vs x_f for different values of B_a/B_{ss}. Similar results are also observed in sample S2.

The break in the induction profile at x_f, which marks changes in the bulk current density and in the relaxation

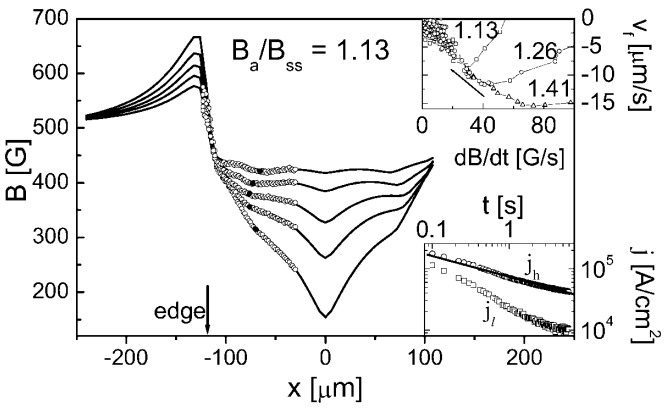

FIG. 3. Time evolution of the magnetic induction profiles for field $H_a = 510$ Oe ($B_a = 430$ G, $B_a/B_{ss} = 1.13$), for sample S1. Profiles shown are measured at $t = 0.14$, 0.3, 0.66, 1.3, and 5.94 s. Bold circles denote the location x_f of the breaks in the profiles. Solid lines are theoretical fits. Lower inset: Log-log plot of $j_h(t)$ and $j_l(t)$. Solid line: Fit of power law for $j_h(t)$, with an exponent -0.34. Upper inset: v_f vs $(dB/dt)_{x=x_f}$ for the indicated ratios B_a/B_{ss}. Arrow indicates direction of time.

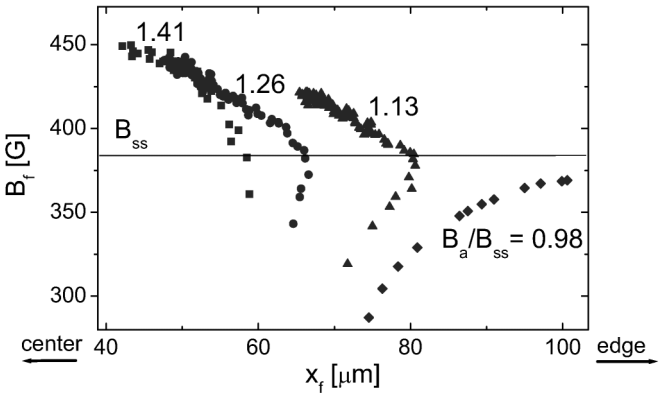

FIG. 4. The time evolution of B_f vs x_f for sample S1 at the indicated values of B_a/B_{ss}. x_f is measured from the center.

characteristics, indicates a dynamic coexistence of two distinct vortex states on both sides of x_f. The identification of these states, and the explanation for the different modes of motion of x_f, become apparent considering the following model.

The premise of the proposed model is that the *sudden* injection of vortices into the sample through its edges creates a transient disordered state of the vortex matter. A similar metastable disordered vortex phase, injected by transport current, was assumed by Paltiel *et al.* [20] to explain a number of puzzling observations in $NbSe_2$. This metastable disordered state has been ascribed to surface imperfections and/or surface barriers which impede "smooth" entrance of the injected fluxons [20]. On the basis of this premise, all of our observations described above find a simple interpretation.

Subsequent to the flux injection and the creation of the transient disordered state, a quasiordered vortex state starts to nucleate near the sample center where the field is minimum. The growth of this state, as dictated by the thermodynamic conditions, leads to the coexistence of two states with different characteristics: a quasiordered state in the sample interior and a disordered state near the edges. The observed break in the profile at x_f marks the border between these two phases. Consistently with this picture we observe larger persistent currents and slower relaxation near the edges, indicating a disordered state.

The monotonic motion of x_f toward the edges for $B_a < B_{ss}$ (Fig. 2 and the right-hand curve in Fig. 4) is now well understood. Since in this case B_f is always smaller than B_{ss}, the front of the quasiordered state at x_f progressively moves toward the sample edges, to create a quasiordered state throughout the entire sample, as dictated by the thermodynamic conditions. When the front reaches the sample edge, the break disappears, indicating that the entire sample is in a quasiordered state. The nonmonotonic behavior of x_f for $B_a > B_{ss}$ (Fig. 3 and the three left-hand curves in Fig. 4) can be explained in a similar way. Initially, B_f is smaller than B_{ss}, and therefore, the ordered state expands toward the edges. However, as B_f approaches B_{ss}, this expansion comes to an halt, as dictated by thermodynamics. Evidently, due to magnetic relaxation, the induction in the region ($|x| < x_f$) occupied by the quasiordered phase continuously increases. As a result, the quasiordered phase starts to retreat and the disordered phase gradually penetrates into the sample. This is manifested by the movement of the break point x_f toward the sample center. When the break reaches the sample center, it disappears, indicating that the entire sample is in a disordered state. It is important to note that the data of Figs. 3 and 4 indicate that an ordered state may persist temporarily above B_{ss}, as it takes time for the disordered state to take over. During this time, as the flux creep process continues, the number of vortices in the system increases and inevitably the induction B_f at the border between the two phases increases.

In the above experiments we followed the growth of the thermodynamic vortex states. We turn now to discuss the growth rates, measured as the velocity of the front $v_f = (dx_f/dt)$. As we show below, the growth rate of the quasiordered state is mainly controlled by the proximity of B_f to B_{ss}, whereas the growth rate of the disordered state is mainly controlled by the dynamics, i.e., by the creep rate.

In the upper inset of Fig. 2 we show the velocity v_f as a function of the induction B_f at the front, accumulated from different experiments in sample S2, corresponding to the indicated ratios B_a/B_{ss}. The figure shows that the velocity decreases monotonically to zero as B_f increases. Moreover, the figure shows that the various $v_f(B_f)$ curves converge as B_f increases, indicating that the growth rate of the ordered phase is limited by the induction increase. We expect the velocity to decrease to zero as B_f approaches B_{ss}. The solid line in this figure is a fit of the data to $v_f \propto (1 - B_f/B_{ss})^{\beta}$ with $\beta = 3.75$ and $B_{ss} = 460$ G, consistent with the measured onset induction of the second magnetization peak for this sample. The decrease in the velocity as a result of the increase in the induction is understood in the following way. Clearly, a growth of the ordered state must be accompanied by retreat of the transient disordered state. As the induction of the transition, B_{ss}, is approached, the free energies of the quasiordered and the disordered states become comparable, and therefore the lifetime of the transient disordered phase becomes larger [20] and diverges with a "critical" exponent β. On the basis of this interpretation one can also understand the absence of traces of the transient disordered state in the data of Fig. 1: Since B_a in this figure is well below B_{ss}, the lifetime of the transient state is shorter than our time resolution. In order to observe the transient state, the field must be raised to values closer to B_{ss}.

The growth rate of the thermodynamic disordered state can be characterized by the velocity of the front x_f after the "turning point" in B_f vs x_f curves, where the movement of x_f changes direction (i.e., x_f starts moving toward the sample center; see the three left curves in Fig. 4). Unlike the situation for $B_f < B_{ss}$ where the increase of B_f toward B_{ss} is the main factor limiting the growth of the ordered

state, for $B_f > B_{ss}$ the induction increase is in favor of the growth of the disordered state. Yet, the growth rate of the disordered state decreases with time, implying that this growth becomes dominantly limited by the flux entry rate. Indeed, contrary to the situation for $B_f < B_{ss}$, in this case plots of v_f vs B_f do not converge. Instead, plots of v_f vs $(dB/dt)_{x=x_f}$ do converge as shown in the upper inset of Fig. 3.

In conclusion, we have described experiments that allow, for the first time, direct observation of the transient disordered vortex state injected into a superconducting sample as a result of an abrupt exposure of the sample to a magnetic field. Our high temporal resolution magneto-optical system reveals that both the quasiordered and the disordered thermodynamic vortex states are preceded by this transient disordered state. For induction steps $B_a < B_{ss}$, the decay of the transient state and the growth of the ordered state progress simultaneously. The rate of this process decreases as the induction increases toward B_{ss}. A markedly different behavior is observed for $B_a > B_{ss}$. In this case, the initial expansion of the quasiordered state stops and the growth of the thermodynamic disordered state assisted by the flux entrance takes over. This is marked by a sharp change in the direction of motion of the boundary between these two phases. The field at the boundary when this change of direction occurs is identified as the thermodynamic transition field B_{ss}. The data clearly show that as *transient* states, a disordered phase may exist below B_{ss} and an ordered state may exist above B_{ss}.

We acknowledge useful discussions with L. Burlachkov, B. Ya. Shapiro, V. K. Vlasko-Vlasov, and E. Zeldov. Special thanks go to L. A. Dorosinskii, B. Mandel, Y. Radzyner, and Y. Wolfus for their help. We thank E. Zeldov for providing us with a preprint of Ref. [20]. This research was supported by The Israel Science Foundation founded by the Israel Academy of Sciences and Humanities-Center of Excellence Program, and by the Heinrich Hertz Minerva Center for High Temperature Superconductivity. Y. Y. acknowledges support from the U.S.-Israel Binational Science Foundation. D. G. acknowledges support from the Clore Foundation. T. T. acknowledges support from a Grant-in-Aid for Scientific Research from the Ministry of Education, Science, Sports, and Culture, and by CREST.

[1] R. Cubitt, E. M. Forgan, G. Yang, S. L. Lee, D. M. Paul, H. A. Mook, M. Yethiraj, P. H. Kes, T. W. Li, A. A. Menovsky, Z. Tarnawski, and K. Mortensen, Nature (London) **365**, 407 (1993).

[2] S. L. Lee, P. Zimmermann, H. Keller, M. Warden, I. M. Savic, R. Schauwecker, D. Zech, R. Cubitt, E. M. Forgan, P. H. Kes, T. W. Li, A. A. Menovsky, and Z. Tarnawski, Phys. Rev. Lett. **71**, 3862 (1993).

[3] V. N. Kopylov, A. E. Koshelev, I. F. Schegolev, and T. G. Togonidze, Physica (Amsterdam) **170C**, 291 (1990).

[4] N. Chikumoto, M. Konczykowski, N. Motohira, and A. P. Malozemoff, Phys. Rev. Lett. **69**, 1260 (1992).

[5] T. Tamegai, Y. Iye, I. Oguro, and K. Kishio, Physica (Amsterdam) **213C**, 33 (1993).

[6] Y. Yeshurun, N. Bontemps, L. Burlachkov, and A. Kapitulnik, Phys. Rev. B **49**, R1548 (1994).

[7] B. Khaykovich, E. Zeldov, D. Majer, T. W. Li, P. H. Kes, and M. Konczykowski, Phys. Rev. Lett. **76**, 2555 (1996).

[8] V. K. Vlasko-Vlasov *et al.*, in *Physics and Materials Science of Vortex States, Flux Pinning and Dynamics*, edited by R. Kossowsky *et al.*, NATO ASI, Ser. E, Vol. 356 (Kluwer, Kordrecht, 1999), p. 205.

[9] N. Motohira *et al.*, J. Ceram. Soc. Jpn. **97**, 994 (1989).

[10] D. Giller, A. Shaulov, R. Prozorov, Y. Abulafia, Y. Wolfus, L. Burlachkov, Y. Yeshurun, E. Zeldov, V. M. Vinokur, J. L. Peng, and R. L. Greene, Phys. Rev. Lett. **79**, 2542 (1997).

[11] V. K. Vlasko-Vlasov, L. A. Dorosinskii, M. V. Indenbom, V. I. Nikitenko, Y. A. Osipyan, and A. A. Polyanskii, Sov. J. Low Temp. Phys. **17**, 762 (1991).

[12] M. V. Indenbom, H. Kronmuller, T. W. Li, P. H. Kes, and A. A. Menovsky, Physica (Amsterdam) **222C**, 203 (1994).

[13] E. Zeldov, A. I. Larkin, V. B. Geshkenbein, M. Konczykowski, D. Majer, B. Khaykovich, V. M. Vinokur, and H. Shtrikman, Phys. Rev. Lett. **73**, 1428 (1994).

[14] Exponential decay of $j_b(t)$ implies nondiverging activation energy $U(j)$ as j approaches zero. We discuss this point elsewhere.

[15] Using the Biot-Savart law, the normal component of the induction is expressed as a function of a surface current density j_s and bulk current density $j(x)$ which is equal to j_l for $|x| < x_f$, j_h for $x_f < |x| < w/2$, and zero for $|x| > w/2$. Fitting this expression to induction profiles measured at different times yields the time dependence of j_s, j_l, j_h, and x_f.

[16] G. Blatter, M. V. Feigelman, V. B. Geshkenbein, A. I. Larkin, and V. M. Vinokur, Rev. Mod. Phys. **66**, 1125 (1994).

[17] Y. Yeshurun, A. P. Malozemoff, and A. Shaulov, Rev. Mod. Phys. **68**, 911 (1996).

[18] M. P. A. Fisher, Phys. Rev. Lett. **62**, 1415 (1989).

[19] A. E. Khalil, Phys. Lett. A **246**, 353 (1998).

[20] Y. Paltiel, E. Zeldov, Y. N. Myasoedov, H. Shtrikman, S. Bhattacharia, M. J. Higgins, Z. L. Xiao, E. Y. Andrei, P. L. Gammel, and D. J. Bishop, Nature (London) **403**, 398 (2000).